



FL3, a Synthetic Flavagline and Ligand of Prohibitins, Protects Cardiomyocytes via STAT3 from Doxorubicin Toxicity

Rehana Qureshi, Onur Yildirim, Adeline Gasser, Christine Basmadjian, Qian Zhao, Jean-Philippe Wilmet, Laurent Désaubry, Canan G Nebigil

► To cite this version:

Rehana Qureshi, Onur Yildirim, Adeline Gasser, Christine Basmadjian, Qian Zhao, et al.. FL3, a Synthetic Flavagline and Ligand of Prohibitins, Protects Cardiomyocytes via STAT3 from Doxorubicin Toxicity. PLoS ONE, 2015, 10 (11), pp.e0141826. 10.1371/journal.pone.0141826 . hal-02391039

HAL Id: hal-02391039

<https://hal.science/hal-02391039>

Submitted on 30 May 2024

HAL is a multi-disciplinary open access archive for the deposit and dissemination of scientific research documents, whether they are published or not. The documents may come from teaching and research institutions in France or abroad, or from public or private research centers.

L'archive ouverte pluridisciplinaire **HAL**, est destinée au dépôt et à la diffusion de documents scientifiques de niveau recherche, publiés ou non, émanant des établissements d'enseignement et de recherche français ou étrangers, des laboratoires publics ou privés.



Distributed under a Creative Commons Attribution 4.0 International License

RESEARCH ARTICLE

FL3, a Synthetic Flavagline and Ligand of Prohibitins, Protects Cardiomyocytes via STAT3 from Doxorubicin Toxicity

Rehana Qureshi¹✉, Onur Yildirim¹✉, Adeline Gasser¹, Christine Basmadjian², Qian Zhao², Jean-Philippe Wilmet¹, Laurent Désaubry^{2,3*}, Canan G. Nebigil^{1*}

1 GPCRs in cardiobiology and Metabolism team, UMR 7242, CNRS–University of Strasbourg, LabEx Medalis, Strasbourg School of Biotechnology, Illkirch, France, **2** Laboratory of Therapeutic Innovation (UMR 7200), Faculty of Pharmacy, University of Strasbourg–CNRS, Illkirch, France, **3** Sino-French Joint Lab of Food Nutrition/Safety and Medicinal Chemistry, College of Biotechnology, Tianjin University of Science and Technology, Tianjin, 300457, China

✉ These authors contributed equally to this work.

* desaubry@unistra.fr (LD); nebigil@unistra.fr (CGN)



OPEN ACCESS

Citation: Qureshi R, Yildirim O, Gasser A, Basmadjian C, Zhao Q, Wilmet J-P, et al. (2015) FL3, a Synthetic Flavagline and Ligand of Prohibitins, Protects Cardiomyocytes via STAT3 from Doxorubicin Toxicity. PLoS ONE 10(11): e0141826. doi:10.1371/journal.pone.0141826

Editor: Partha Mukhopadhyay, National Institutes of Health, UNITED STATES

Received: March 31, 2015

Accepted: October 13, 2015

Published: November 4, 2015

Copyright: © 2015 Qureshi et al. This is an open access article distributed under the terms of the [Creative Commons Attribution License](https://creativecommons.org/licenses/by/4.0/), which permits unrestricted use, distribution, and reproduction in any medium, provided the original author and source are credited.

Data Availability Statement: All relevant data are within the paper.

Funding: This work was supported by the "Association pour la Recherche sur le Cancer" (ARC, grant numbers 3940, SF120111204054 and PJA 20141201909) and the "Agence Nationale la Recherche" (ANR, grant number ANR-11-EMMA-021). This work has also been published within the LABEX ANR-10-LABX-0034_Medalis and received a financial support from the French government managed by Agence Nationale de la recherche under Programme d'investissement d'avenir. Christine

Abstract

Aims

The clinical use of doxorubicin for the treatment of cancer is limited by its cardiotoxicity. Flavaglines are natural products that have both potent anticancer and cardioprotective properties. A synthetic analog of flavaglines, FL3, efficiently protects mice from the cardiotoxicity of doxorubicin. The mechanism underlying this cardioprotective effect has yet to be elucidated.

Methods and Results

Here, we show that FL3 binds to the scaffold proteins prohibitins (PHBs) and thus promotes their translocation to mitochondria in the H9c2 cardiomyocytes. FL3 induces heterodimerization of PHB1 with STAT3, thereby ensuring cardioprotection from doxorubicin toxicity. This interaction is associated with phosphorylation of STAT3. A JAK2 inhibitor, WP1066, suppresses both the phosphorylation of STAT3 and the protective effect of FL3 in cardiomyocytes. The involvement of PHBs in the FL3-mediated cardioprotection was confirmed by means of small interfering RNAs (siRNAs) targeting PHB1 and PHB2. The siRNA knockdown of PHBs inhibits both phosphorylation of STAT3 and the cardioprotective effect of FL3.

Conclusion

Activation of mitochondrial STAT3/PHB1 complex by PHB ligands may be a new strategy against doxorubicin-induced cardiotoxicity and possibly other cardiac problems.

Introduction

Anthracyclines (e.g., doxorubicin) remain a mainstay therapy for cancers such as leukemias, lymphomas, and breast and gastric cancers, even though these compounds cause substantial cardiotoxicity that can ultimately lead to congestive heart failure [1]. Therefore, approaches to

Basmadjian and Qian Zhao were supported by AAREC Folia Research and the Association Nationale de la Recherche et de la Technologie. Onur Yildirim received an Erasmus fellowship. This work was supported by grants from Centre National de la Recherche Scientifique, and Université de Strasbourg. The funders had no role in study design, data collection and analysis, decision to publish, or preparation of the manuscript.

Competing Interests: The authors have declared that no competing interests exist.

alleviation of the cardiotoxic effects of doxorubicin are urgently needed in oncology. Dexrazoxane, which is the only clinically approved cardioprotectant against anthracycline cardiotoxicity, had been shown to induce secondary tumors and was consequently removed from the European market [2]. Thus, there is a need for efficacious and safe drugs that can protect cancer patients from the cardiotoxicity of anthracyclines.

Flavaglines are natural products isolated from Chinese medicinal plants that have potent anticancer effects without toxicity to healthy tissues [3]. Not only are flavaglines specifically toxic to cancer cells, but they also promote the survival of neurons, T lymphocytes, and cardiomyocytes under conditions of adverse effects of chemotherapeutic agents: cisplatin, etoposide, and doxorubicin respectively [4–6]. In particular, in a previous study, we found that a synthetic flavagline, FL3, almost doubles the survival rate of mice (56% treated versus 31% untreated) in an *in vivo* model of doxorubicin-induced acute cardiotoxicity [4]. Recently, we also showed that flavaglines directly bind to prohibitins (PHBs) in cancer cells [7]. PHBs are scaffold proteins that exist in two isoforms: PHB1 and PHB2 [8]. PHBs seem to perform a function in cancer cells that is different from that in healthy cells: PHBs may be located in several compartments, but they are mainly concentrated in mitochondria in healthy cells and in the nucleus in cancer cells [8]. This divergence of cellular localization (and possibly function) may explain why flavaglines promote apoptosis in cancer cells and survival in healthy cells.

PHB1 has been shown to prevent mitochondrial dysfunction via activating STAT3 in intestinal epithelium (as reviewed elsewhere [9]), but whether this event occurs in cardiomyocytes remains unreported. STAT3 phosphorylation [10] and overexpression [11] have been shown to protect the heart from doxorubicin-induced cardiotoxicity. Moreover, cardiac-restricted deletion of STAT3 increases the susceptibility to doxorubicin-induced heart failure [12, 13].

In this study our aim was to determine whether flavaglines exert their cardioprotective effect by modulating PHB1 localization and activating STAT3 signaling.

Methods

Cell culture

The H9c2 cardioblast cell line that was derived from an embryonic rat heart was obtained from American Type Culture Collection (Manassas, VA, USA). The cells were grown in Dulbecco's modified Eagle's medium (DMEM) supplemented with 10% fetal calf serum at 37°C in a humidified atmosphere containing 5% CO₂. The medium was changed every 2–3 days.

The *in vitro* cardiotoxicity assay

H9c2 cells were plated and grown for 24 h in 100-mm culture dishes at $7 \times 10^3/\text{cm}^2$. Next, the cells were washed and cultured for 12 h in a glucose-free medium (Gibco; DMEM with L-glutamine, without D-glucose and sodium pyruvate) supplemented with only 1% fetal calf serum. The cells were pretreated with FL3 (100 nM) under serum-free conditions for 10 h, and then either doxorubicin (1 μM) or vehicle alone (DMSO) was added to the medium for additional incubation for 14 h. The doxorubicin concentration and incubation time were chosen in accordance with a known model of acute cardiotoxicity [14]. The H9c2 cardiomyocytes were preincubated with WB1066 (1 μM) for 1 h before FL3 treatment. The cells were then washed, and either terminal deoxynucleotidyl transferase dUTP nick end labeling (TUNEL) or fluorescence-activated cell sorting (FACS) analysis was performed.

Detection and quantification of apoptosis

Terminal deoxynucleotidyl transferase dUTP nick end labeling (TUNEL) assays of fragmented DNA was performed according to the manufacturer's instructions (Millipore) [4]. Cells were fixed in 4% formaldehyde, permeabilized. The cells were incubated with TdT terminal transferase and fluorescein-dUTP. Then, the cells were counterstained with 4',6-diamidino-2-phenylindole (DAPI). The TUNEL labeling index was calculated as the percentage of DAPI-stained TUNEL-positive cells among total DAPI-labeled cells by viewing each visual field at 40× magnification. Generally, 10 different visual fields containing around 20 cells were analyzed in each sample, and each experiment was repeated at least three times.

Apoptosis was also analyzed by FACS analysis (FACSCalibur, Becton-Dickinson Biosciences, Le Pont De Claix, France). We harvested 7×10^3 cells and washed them with "annexin binding buffer" (0.01 M HEPES, 0.14 M NaCl, 2.5 mM CaCl_2) and labeled the cells with annexin V (dilution 1:50) and Topo (6.7 $\mu\text{g}/\text{mL}$). All assays were performed at least in triplicate, and the results were analyzed in the BD Cell Quest Pro software (Becton-Dickinson Biosciences).

Pull-down assay

This assay was performed by means of FL3-Affigel as described previously [7]. One hundred million H9c2 cells were washed in PBS and lysed in 2 mL of a lysis buffer consisting of 50 mM Tris-HCl pH 8.0, 120 mM NaCl, 1% NP-40, 5 mM dithiothreitol (DTT), 200 μM Na_3VO_4 , 25 mM NaF, and a protease inhibitor cocktail (Roche Diagnostics, Switzerland). Cellular debris were removed by centrifugation at $10\,000 \times g$ for 30 min. Five hundred micrograms of total protein extract was incubated for 12 h at 4°C with 40 μL of FL3-Affigel, negative control (NC)-coupled beads, or uncoupled Affi-Gel beads. The beads were extensively washed with the lysis buffer, and the bound proteins were eluted and reduced in a sample buffer consisting of 63 mM Tris-HCl pH 6.8, 2% SDS, 10% glycerol, a trace of bromophenol blue (0.05%), and 200 mM DTT for 30 min at 65°C. After cooling on ice, each sample was alkylated with a final concentration of 150 mM iodoacetamide for additional 30 min. The proteins were separated by SDS-PAGE (10% gel; Bio-Rad Laboratories, USA) and western blot analyses were performed using anti-PHB1 and anti-PHB2 antibodies.

Immunohistochemical analysis

H9c2 cells were plated and grown for 24 h in Labtek-8 dishes at the density 2×10^4 /well in an incubator with 5% CO_2 at 37°C. The medium was changed to DMEM containing 2% fetal calf serum for starvation of the cells for 24 h. After the starvation procedure, the cells were pre-treated with MitoTracker Red CMXRos (Life Technologies) for 1 h, then treated with 0.1% dimethyl sulfoxide (DMSO) as a vehicle or FL3 (100 nM) for 0, 5, 10, 15, 30, 45, or 60 min. After that, the cells were fixed with 3.7% (v/v) formaldehyde for 15 min at room temperature and incubated with a blocking solution consisting of 5% BSA (bovine serum albumin) and 1% Triton X-100 in PBS at room temperature for 1 h. The cells were incubated with the anti-PHB1 antibody at 4°C overnight and then incubated for 1 h with an Alexa Fluor 488-conjugated anti-rabbit IgG antibody (Life Technologies/Molecular Probes) [15]. The cells were mounted on slides with the Vectashield Mounting Medium (Vector Labs) and DAPI for counterstaining of the nucleus. The cell images were acquired using a Leica TCS SP5 Confocal Microscopy System (Leica M, Germany) equipped with a 63×/1.40 NA oil-immersion objective lens. The images were captured at the scanning speed of 400 Hz and image resolution 512×512 pixels and were then analyzed using the Leica Application Suite, Advanced Fluorescence (LAS AF) software.

Plasmid transfection

The PE935 (PHB1-Flag) and PE936 (PHB2-Flag) plasmids were transfected into H9c2 cells using Jet Prime (POL114-07, PolyPlus Transfection). The cells at 60–80% confluence in a 60-cm² culture plate were incubated with an antibiotic-free medium. Twelve micrograms of plasmid DNA was used for the transfection. Forty-eight hours after the transfection, the FLAG-PHB1 and FLAG-PHB2 proteins were purified from the transfectant H9c2 cells by immunoprecipitation using an anti-FLAG antibody and FLAG-peptide elution.

Protein purification by immunoprecipitation

Immunoprecipitation of PHBs with the anti-FLAG antibody from the transfectant H9c2 cells was performed as described previously [7]. The H9c2 cells were incubated for 0, 15, or 30 min with FL3 (Enzo Life Sciences). Subsequently, the cells were washed in ice-cold PBS, lysed in the IP buffer (20 mM Tris-HCl, 5 M NaCl, 2 mM EDTA, 1% Triton X-100, and protease inhibitors) and centrifuged (10 000 × g, 20 min) to clear the lysates. Aliquots were taken for input control, and the lysates were incubated with protein G Plus/A-agarose beads (#IP10, Calbiochem) for 30 min at 4°C, then overnight with an anti-FLAG antibody (anti-FLAG M2, Sigma-Aldrich, St. Louis, MO, USA; cat. # F1804). After that, the immunoprecipitates were washed with a lysis buffer (1% NP-40, 300 mM NaCl, 10% glycerol, 10 mM Tris-HCl pH 7.5), then a buffer without salt (1% NP-40, 10% glycerol, 10 mM Tris pH 7.5), and centrifuged for 10 min at 20 000 rpm and 4°C. Next, the samples were boiled in a denaturing sample buffer at 95°C for 5 min. The binding of STAT3 to the PHB1 proteins was detected by western blot analyses using anti-STAT3 or anti-phospho-STAT3 antibodies (Cell Signaling).

Subcellular fraction of H9c2 cells and the STAT3 phosphorylation assay via western blotting

H9c2 cells were plated and grown for 24 h. Next, the cells were washed and cultured for 12 h in the above-mentioned glucose-free medium, supplemented with only 1% fetal calf serum. The cells were then incubated with either FL3 or vehicle alone (0.1% DMSO) for 0, 5, 10, 15, or 30 min and harvested with a lysis buffer (50 mM Tris-HCl pH 7.0, 1 mM EDTA, 100 mM NaCl, 0.1% SDS, 1% NP-40, 1 mM Na₃VO₄, 1 mg/mL aprotinin, 1 mg/mL pepstatin, and 1 mg/mL leupeptin). The whole-cell lysates were centrifuged at 12 000 × g for 15 min at 4°C. The cell debris was removed.

Cytoplasmic and mitochondrial fractions from cultured cells were prepared using Subcellular Protein Fractionation Kit for Cultured Cells (Thermo Scientific) and nuclear isolation kit, employing the nuclear protein extraction buffer (20 mM Tris-HCl, pH 7.6, 50 mM KCl, 400 mM NaCl, 1 mM EDTA, 0.2 mM PMSF, 5 mM β-mercaptoethanol, aprotinin (1000 U/ml), 1% Triton X-100, and 20% glycerol as described [16]. 30 μg of total protein, 5 μg or 10 μg of cytosolic, mitochondrial proteins or nuclear protein were used for Western blot analyses. The proteins were separated under denaturing conditions using SDS-PAGE (10% gel) and transferred to a polyvinylidene difluoride (PVDF) membrane. The blots were incubated with a blocking solution consisting of a 5% solution of a fat-free milk powder in PBS-T (PBS plus Tween 20, 0.1%) at room temperature for 1 h. After three washes with PBS-T for 10 min, the blots were incubated overnight at 4°C with gentle shaking with a primary antibody anti-phospho-STAT3 antibody Ser (727) (Cell Signaling), (1:500 dilution in PBS-T containing 0.5% of the fat-free milk powder) or PHB1 (Cell Signaling).

After three washes with PBS-T, the membrane was incubated for 1 h at room temperature with gentle shaking with a horseradish peroxidase-conjugated goat anti-IgG antibody (1:1000

dilution) in PBS-T containing 0.5% of the fat-free milk powder. The expected bands were visualized after 5-min incubation to induce enzyme-linked chemiluminescence (GE HealthCare), and then the blots were washed, stripped, and reprobed with a Total -STAT3 antibody (Cell Signaling) or vinculin (Cell Signaling) or actin (Santa Cruz) as internal control, followed by incubation with a suitable secondary antibody. The phospho-STAT3 or PHB1 signals were quantified by scanning laser densitometry and normalized to total amounts of the corresponding STAT3 or vinculin protein, respectively.

Transfection with small interfering RNA (siRNA)

A 50-nM solution of siRNA against rat PHB2 (Ambion; siRNA #258474) or a mixture (10 nM each) of siRNAs against rat PHB2 and PHB1 (Ambion, USA; siRNA #199561) were used for transfection of 90%- to 95%-confluent cells in a serum-free medium. Nonspecific siRNA (Ambion) served as a negative control. The transfection was based on Lipofectamine 2000 (Invitrogen, USA), according to the manufacturer's instructions. Forty-eight hours after the transfection, the PHB1 levels were measured by quantitative PCR and western blot analysis.

Statistical analysis

All samples were prepared (and used in experiments) at least in triplicate. The results of the quantitative experiments were expressed as mean \pm SEM. Multigroup comparisons were performed using one-way analysis of variance (ANOVA) with *post hoc* Bonferroni's correction. Comparisons between two groups were conducted using unpaired Student's *t* test. In all analyses, $p < 0.05$ was assumed to denote statistical significance. All calculations were performed in the Prism software.

Results

FL3 binds to PHB1 and PHB2 in cardiomyocytes

To test whether FL3 binds to PHBs in cardiomyocytes, we performed a pull-down assay with protein extracts of the H9c2 cardiomyocytes using a biologically active flavagline (FL3) conjugated to Affi-Gel beads [7,17]. Whole-cell extracts from H9c2 cells (input), the bound and eluted proteins (Affi-Gel-FL3), and output proteins (output Affi-Gel-FL3) were subjected to western blot analysis using antibodies against PHB1 and PHB2. Both PHB1 and PHB2 (Fig 1A) were retained by the affinity matrix. The blank beads did not pull down any PHB proteins (lane 4 in Fig 1A). These data showed that PHB1 and PHB2 were the cellular targets of FL3 in the H9c2 cardiomyocytes. Next, we examined whether doxorubicin and/or FL3 modify the content of PHB1 in these cells (Fig 1B and 1C). FL3 treatment of the H9c2 cells for 10h (with or without doxorubicin) greatly augmented PHB1 protein levels. Doxorubicin has no significant effect on PHB1 levels (Fig 1B and 1C), but it induced its accumulation in the nucleus (Fig 1D, 1E and 1F). This translocation of PHB1 from cytoplasm to the nucleus was blocked by FL3 (Fig 1D, 1E and 1F). This data indicate that PHB1 levels and localization can be greatly modified by FL3 treatment.

FL3 promotes the localization of PHB1 to mitochondria

A large body of evidence suggests that the subcellular location of PHBs determines whether a PHB protein promotes apoptosis or cytoprotection [8,18]. Accordingly, we examined the intracellular localization of PHB1 after treatment with FL3 to gain some insight into FL3's mechanism of action. H9c2 cells were double-labeled with an anti-PHB1 antibody and the mitochondrial dye Mitotracker Red. PHB1 was detected throughout the cytoplasm of the H9c2

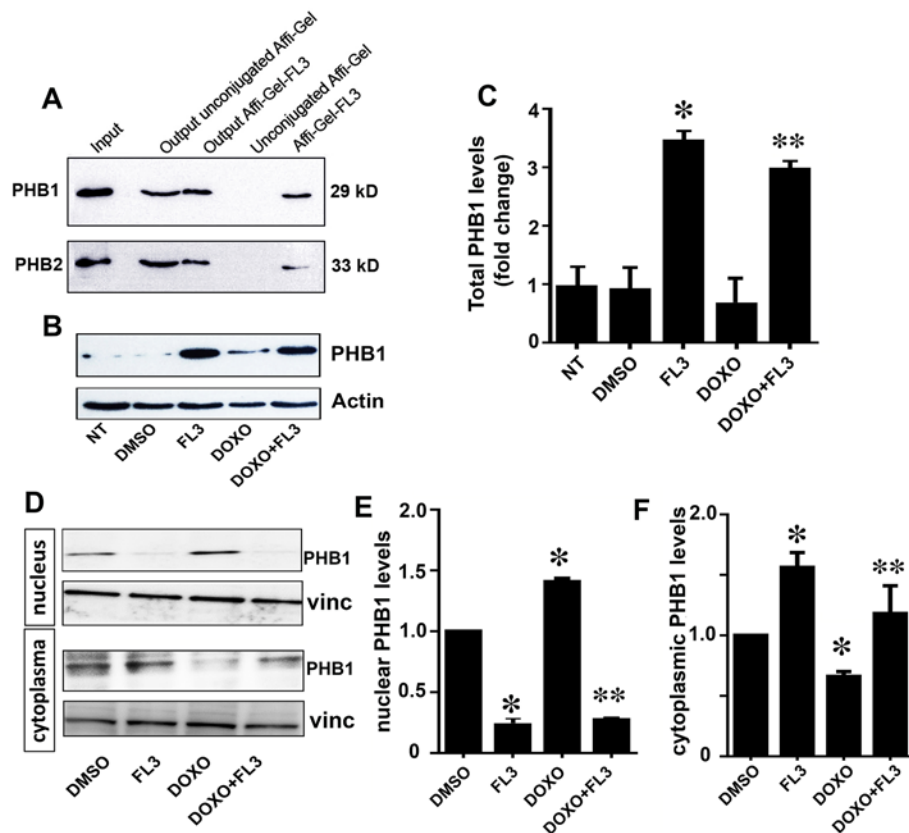


Fig 1. Synthetic flavagline (FL3) binds PHB1 and PHB2 and increases PHB1 levels in H9c2 cells. A. Whole-cell extracts of the H9c2 line (input) were either incubated with the beads Affi-Gel 10 conjugated with FL3 or blocked with ethanolamine (unconjugated Affi-Gel) [7,17]. The bound and eluted proteins (Affi-Gel-FL3) and output proteins (output Affi-Gel-FL3) were analyzed by western blotting using antibodies against PHB1 and PHB2 ($n = 3$). **B and C.** Representative western blot analyses and histogram based quantification of total PHB1 levels in the cell lysates by FL3 alone increased PHB1 protein levels within 10h as compared to non-treated cells (NT). However PHB1 level was lower in the presence of both FL3 and doxorubicin ($n = 3$). **D and E.** Representative western blot analyses and histogram based quantification of nuclear PHB1 levels by doxorubicin accumulates PHB1 in the nucleus but lowers in the cytoplasm that was reduced by preconditioning with FL3. * Indicates $p < 0.05$ as compared to control, ** indicates $p < 0.05$ as compared to the doxorubicin alone group.

doi:10.1371/journal.pone.0141826.g001

cardiomyocytes in the basal condition (Fig 2A). The staining pattern for PHB1 maximally matched that of Mitotracker Red after 15-min incubation of the cells with FL3, indicating that FL3 promoted PHB1 accumulation predominantly in mitochondria (Fig 2B). Mitochondrial fraction of the FL3 treated H9c2 cells confirmed an amplification of PHB1 levels in mitochondria after 15 min (Fig 2C and 2D). PHB1 accumulation in nucleus was elevated within 10 min and was consequently reduced within 20 min upon FL3 treatment (Fig 2C and 2E). This data clearly showed that FL3 promotes nuclear translocation of PHB1 to mitochondria.

FL3 promotes activation of STAT3 by PHB1

FL3 enhanced phosphorylation of STAT3 in mitochondria in a time dependent manner (Fig 3A and 3B) and correlated with PHB1 accumulation in the mitochondria and nucleus (Fig 3C and 3D), indicating that FL3 promotes nuclear translocation of PHB1 to mitochondria and consequently STAT3 phosphorylation. Next we investigated whether PHB1 accumulation and

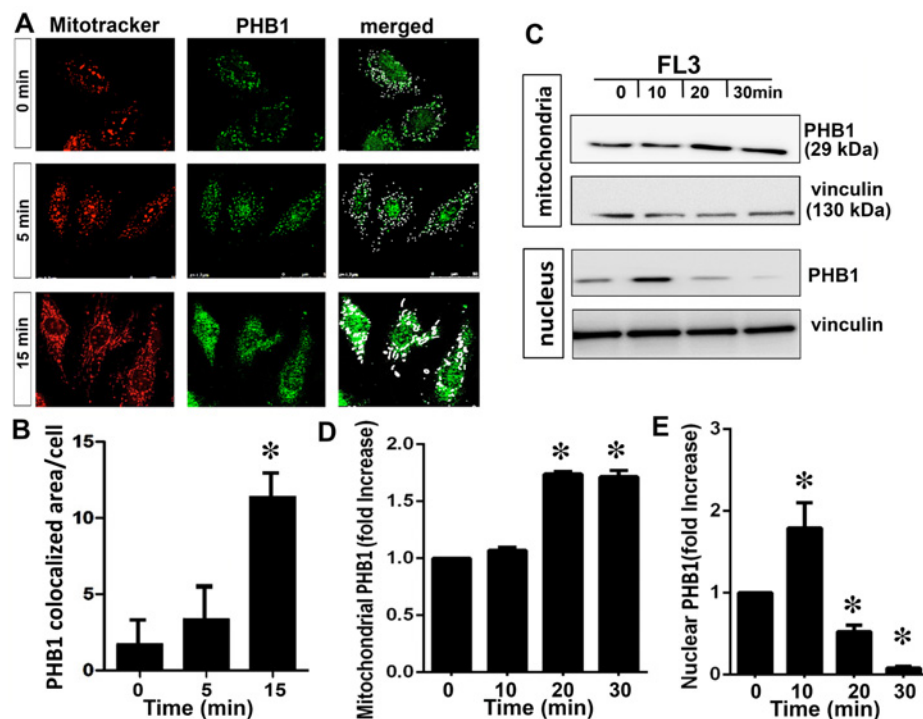


Fig 2. The flavagline FL3 induces translocation of PHB1 to mitochondria in cardiomyocytes. **A.** H9c2 cells were incubated with FL3 (100 nM) and analyzed by confocal microscopy. The cells were co-labeled with the anti-PHB1 antibody (green staining), mitotracker (red staining), and (DAPI; blue staining). The latter two dyes stained mitochondria and the nucleus, respectively. Merged confocal images show that FL3 induced the translocation of PHB1 to mitochondria (white arrows show PHB1 and mitotracker co-localization). **B.** The histogram shows quantitative analyses of co-localization of PHB1 and Mito Tracker in each cell by confocal analyses (n = 6). **C.** Representative illustration of PHB1 levels in mitochondrial and nuclear fractions upon FL3 treatment. In the mitochondrial fraction PHB1 accumulation by FL3 occurred within 20 min. PHB1 was initially increased in nucleus and rapidly reduced within 20 min. **D and E.** The histogram shows quantitative analyses of mitochondrial and nuclear PHB1 levels upon treatment of H9c2 cells with FL3 (100 nM). * Indicates $p < 0.05$ as compare to vehicle (n = 3).

doi:10.1371/journal.pone.0141826.g002

STAT3 phosphorylation are also correlated upon doxorubicin treatment of the H9c2 cells. Accordingly, phosphorylation of nuclear STAT3 is elevated by doxorubicin that was blocked by FL3 preconditioning (Fig 3E and 3F).

Next, we addressed whether FL3 promotes interaction of PHB1 with STAT3 in H9c2 cells, since PHB1 accumulation and STAT3 phosphorylation are correlated in mitochondria and nucleus. Moreover, PHB1 has been shown to heterodimerize with STAT3 [8]. H9c2 cells that were cotransfected with plasmids encoding FLAG-tagged PHB1 and PHB2 were incubated with FL3 (100 nM) for immunoprecipitation of PHBs with an anti-FLAG antibody. The immunoprecipitated cell lysates (input) from the H9c2 cells that were transfected with PHB1 or PHB2 (IP- α -Flag) were subjected to western blot analyses with anti-flag antibodies. Significant coimmunoprecipitation of PHB1 with STAT3 was observed at the data point 15 min after FL3 treatment (Fig 4A, left panels), whereas interactions of PHBs with either AKT or ERK were not detected. These results showed that FL3 induced heterodimerization of STAT3 with PHBs. When the immunoprecipitated PHB1 proteins were visualized with an antibody recognizing the phosphorylated form of STAT3, the phospho-STAT3 was significantly upregulated 15 min after FL3 treatment (Fig 4A, right panels). Taken together, these data suggested that PHBs

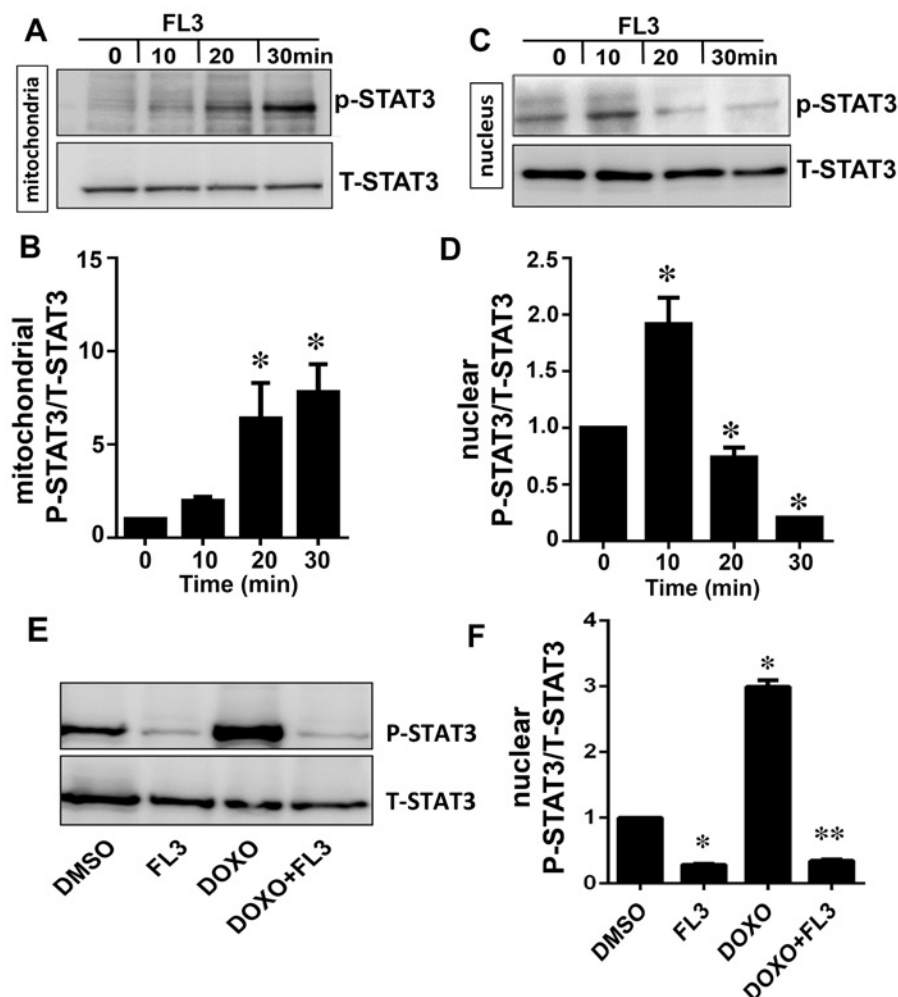


Fig 3. The mitochondrial STAT-3 phosphorylation is correlated with PHB1 translocation to mitochondria by FL3 in cardiomyocytes. **A and B.** Representative western blot analyses and histogram based quantification of mitochondrial STAT3 activation by phosphorylation. STAT3 was phosphorylated by FL3 in mitochondrial fraction. **C and D.** Representative western blot analyses and histogram based quantification of nuclear STAT3 activation by phosphorylation. STAT3 activation was only detected in nucleus after FL3 treatment. **E and F.** The western blot and histogram show quantitative analyses of nuclear phosphorylated STAT3 levels upon treatment of H9c2 cells with control (DMSO), FL3 (100 nM), doxorubicin (1 μ M), and FL3 + doxorubicin. Doxorubicin elevated phosphorylated STAT3 levels, which were reduced by FL3 ($n = 3$; * $p < 0.05$, compared to vehicle; ** $p < 0.05$, compared to doxorubicin treatment).

doi:10.1371/journal.pone.0141826.g003

interacted with the STAT3 protein, and this interaction induced activation of STAT3 by phosphorylation.

Next, we examined STAT3 activation by phosphorylation in H9c2 cells after FL3 treatment. Using a specific anti-phospho-STAT3 antibody and western blot analysis, we found that FL3 (100 nM) rapidly promoted the phosphorylation of STAT3 in the H9c2 cardiomyocytes: the phosphorylation reached a maximum within 15 min (Figs 4B and 3C). To gain further insight into the activation of STAT3 by PHBs, we tested whether the STAT3 phosphorylation is inhibited by WP1066 [19], an inhibitor of the JAK2 kinase (this reagent is commonly used to block STAT3 activation). WP1066 at 100 nM significantly inhibited the FL3-induced STAT3 activation (Figs 4D and 3E).

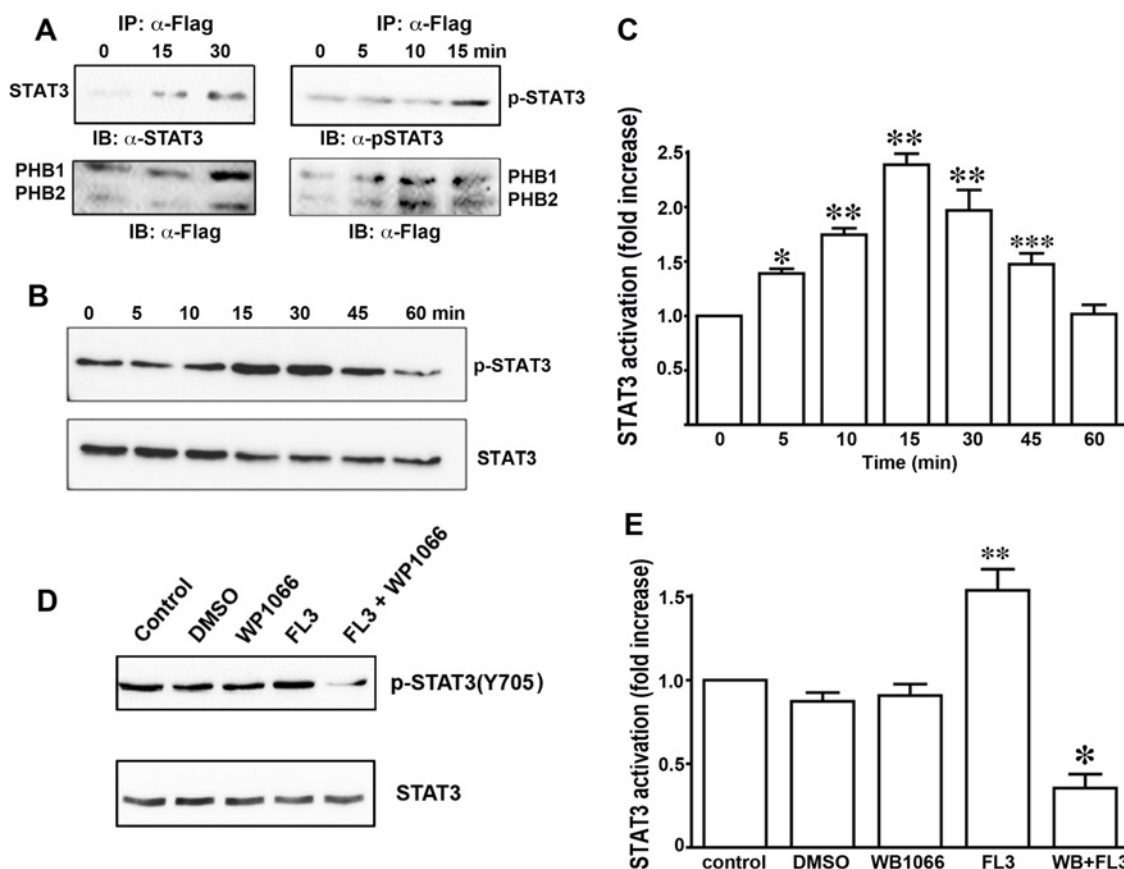


Fig 4. FL3 rapidly induces phosphorylation of STAT3. **A.** STAT3 coimmunoprecipitates (co-IP) with PHB1. An anti-FLAG antibody was incubated with extracts of the H9c2 cardiomyocytes. Immunoprecipitates were resolved by means of SDS-PAGE and probed for STAT3 and the FLAG tag to detect both PHB1 and PHB2. **B.** Representative western blots of protein lysates of H9c2 cells treated with FL3 (100 nM), by means of antibodies that recognize either phosphorylated (Tyr⁷⁰⁵) or total STAT3 protein. **C.** Quantitative analysis of the western blots (percentage of phosphorylated STAT3 in total STAT3, $n = 4$; * $p < 0.05$, compared to control; ** $p < 0.001$, compared to control; *** $p < 0.01$, compared to control). **D** and **E.** Effects of the Janus kinase 2 (JAK2) inhibitor WP1066 on STAT3 phosphorylation: Representative western blots and quantitative analysis (percentage of phosphorylated STAT3 in total STAT3, $n = 4$; $p < 0.05$, compared to control; ** $p < 0.05$, compared to FL3).

doi:10.1371/journal.pone.0141826.g004

FL3 triggers cardioprotective signaling by targeting PHB1 and its signaling

To confirm the involvement of PHBs in the mechanism of action of FL3, we tested whether a knockdown of PHB1 in cardiomyocytes affects the cardioprotective effect of FL3. Accordingly, we transfected the H9c2 cardiomyocytes with siRNAs against PHBs to downregulate PHBs without altering cell survival. Of the two anti-PHB siRNA sequences tested, si-PHB1 at 50 nM or si-PHB1 together with si-PHB2 (10 nM each) downregulated both PHB1 mRNA and protein: by 80% and 70%, respectively. The siRNA-mediated downregulation of PHB1 and PHB2 significantly reduced the cytoprotective effect of FL3 (Fig 5A), whereas transfection with control (nonspecific) siRNA did not. These data indicated that PHB1 and PHB2 were both involved in the mechanism of action of FL3.

To determine whether the STAT3 phosphorylation in cardiomyocytes was indeed involved in the cardioprotective mechanism; we compared the apoptosis levels in TUNEL and FACS assays when the H9c2 cardiomyocytes were pretreated with WP1066 or vehicle alone. The TUNEL

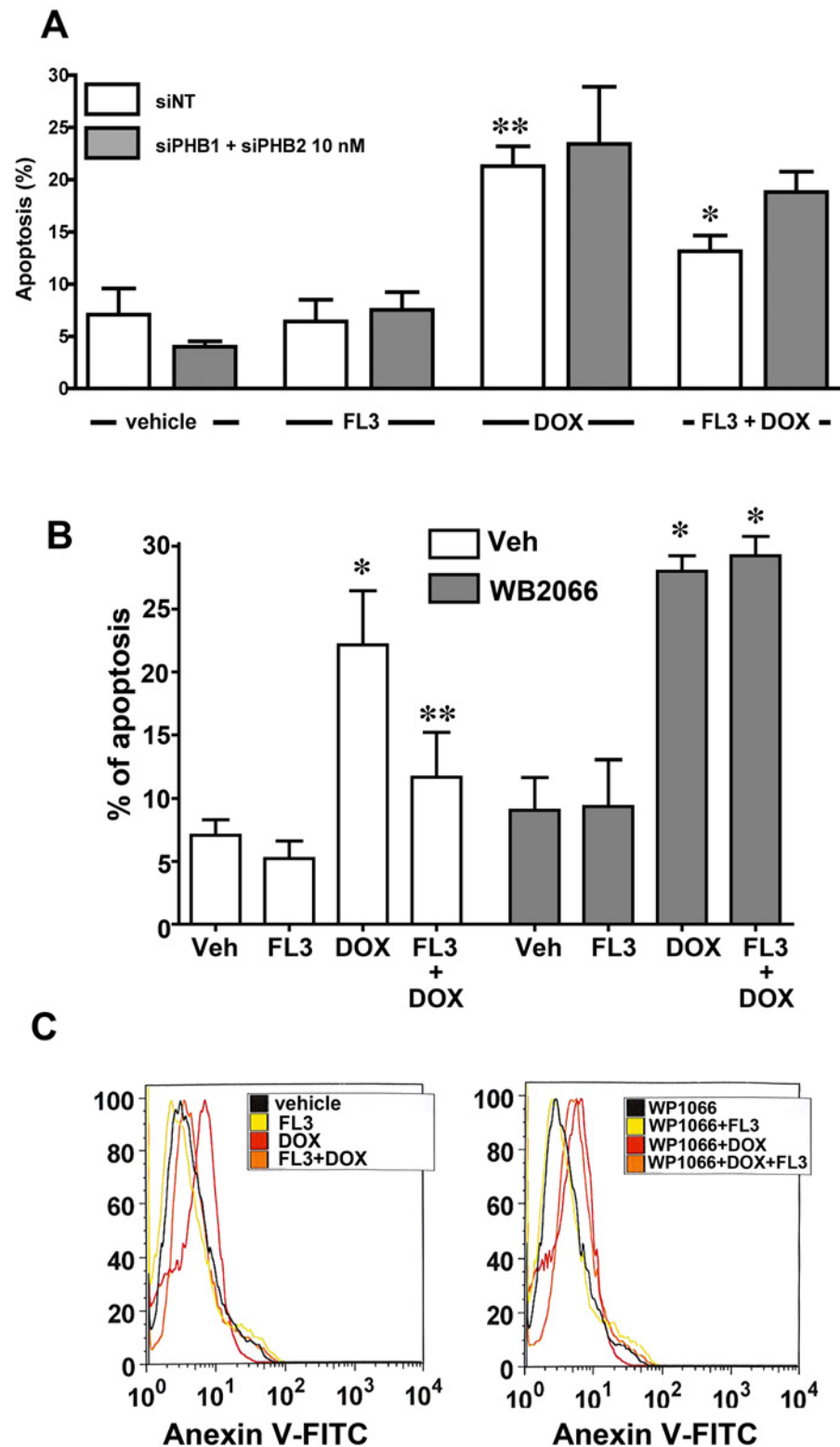


Fig 5. FL3 protects H9c2 cardiomyocytes by acting on PHBs and their signaling target STAT3. A. The histogram shows the percentage of apoptotic cells induced by doxorubicin (1 μ M) among H9c2 control cells (transfected with nonspecific small interfering RNA [si-NT]) or the H9c2 cells where PHB1 or PHB2 were

downregulated using specific small interfering RNA (siRNA). Knocking PHB1 or PHB2 down greatly diminished the cardioprotective effect of FL3 (100 nM; $n = 4$ to 5 ; $*p < 0.05$, compared to vehicle; $**p < 0.05$, compared to doxorubicin (doxo). **B.** The TUNEL assay shows the percentage of apoptotic cells in the 4',6-diamidino-2-phenylindole (DAPI)-positive total cell population. **C.** Fluorescence-activated cell sorting (FACS) analysis shows the percentage of the maximum among annexin V-positive cells ($n = 3$; $*p < 0.05$, compared to vehicle; $**p < 0.05$, compared to doxorubicin treatment).

doi:10.1371/journal.pone.0141826.g005

(Fig 5B) and FACS data (Fig 5C) revealed that WP1066 strongly attenuated the cardioprotective effect of FL3. Overall, these results supported the notion that phosphorylation of STAT3 is a crucial step in the mechanism of cardioprotective action of FL3.

The PHB1/STAT3 complex is a key participant in the FL3-activated STAT3 pathway

To confirm whether the PHB1/STAT3 complex is involved in the FL3-activated STAT3 pathway, we transiently cotransfected the cells with either anti-PHB1 siRNAs or scrambled RNA as a control, then incubated the cells with FL3, and tested them for STAT3 phosphorylation. The anti-PHB1 siRNA, but not scrambled RNA, strongly attenuated the FL3-induced STAT3 phosphorylation (Fig 6A and 6B). The levels of PHBs in siRNA-nontargeted and siRNA-PHBs

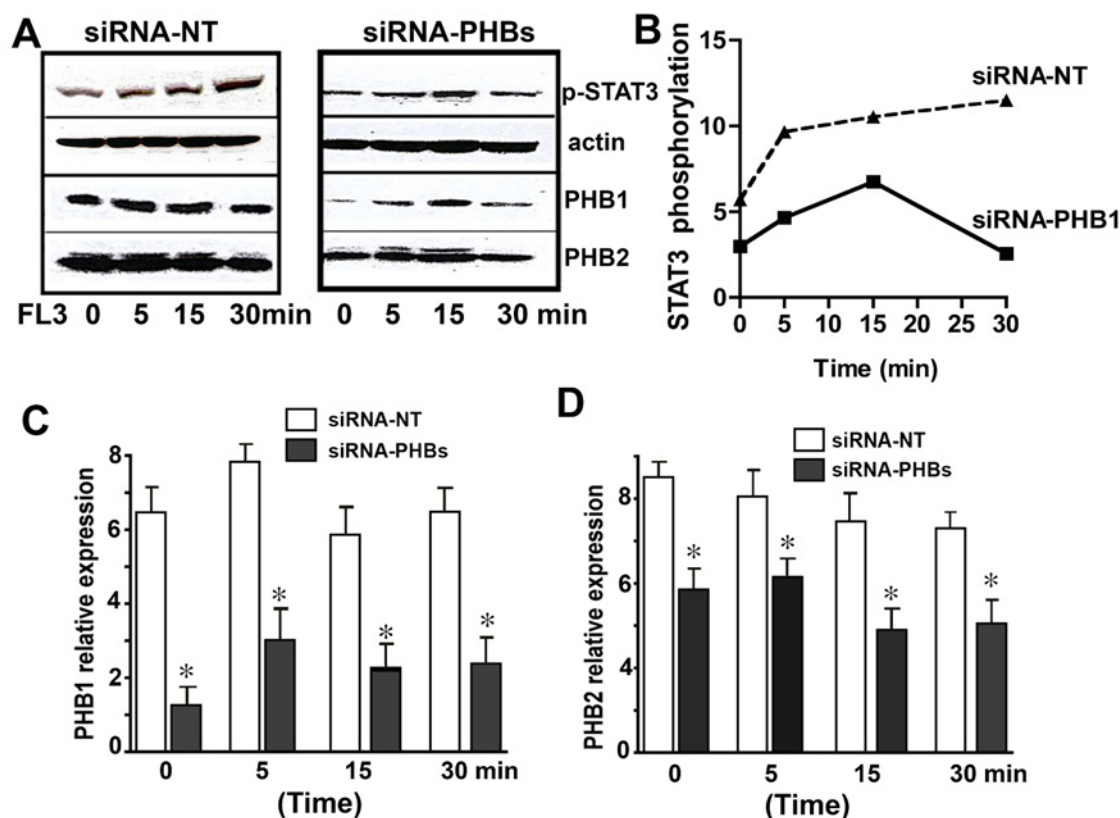


Fig 6. Small-interfering-RNA (siRNA)-mediated downregulation of PHB1 proteins attenuates FL3-induced cardioprotection from doxorubicin toxicity. **A.** Representative western blots show induction of STAT3 phosphorylation by the synthetic flavagline (FL3) in H9c2 cells transfected with nonspecific siRNA (left) or with anti-PHB1 siRNA (right). **B.** Quantification of phosphorylated STAT3, with normalization to actin ($n = 3$; $*p < 0.05$, compared to vehicle). FL3-mediated STAT3 activation by phosphorylation was abolished when the expression of PHBs were reduced. **C.** This histogram shows downregulation of PHB1 after transfection of H9c2 cells with anti-PHBs siRNA ($n = 3$; $*p < 0.05$, compared to vehicle). **D.** This histogram shows downregulation of PHB2 after transfection of H9c2 cells with anti-PHBs siRNA ($n = 3$; $*p < 0.05$, compared to vehicle).

doi:10.1371/journal.pone.0141826.g006

transfected cells are shown in (Fig 6C and 6D). These results showed that PHB1 was necessary for the STAT3 activation by FL3, and that STAT3 was downstream of PHB1 in the FL3-mediated survival pathway.

Discussion

A study on the cardiac phosphoproteome has already shown PHB1 to be a prime target of doxorubicin [20]. Nonetheless, how the PHB proteins participate in the survival mechanisms against doxorubicin-mediated cardiotoxicity was not known. Here, we show for the first time that FL3 binds to PHBs and translocated PHB1 to mitochondria. Accumulation of PHB1 in mitochondria is associated with STAT3 phosphorylation. It seems that mitochondrial PHB1 accumulation stabilizes mitochondrial membrane, activates mitochondrial STAT3 activation and initiates FL3-mediated cardioprotection. On the opposite, doxorubicin provokes the PHB1 accumulation and STAT3 phosphorylation in nucleus, leading to cardiomyocyte apoptosis (Fig 7).

PHB1 has been reported to promote the survival of many noncancerous cell types, including cardiomyocytes [8,21–26]. Overexpression of PHB1 inhibits the mitochondria-mediated apoptosis pathway in H9c2 cells that is induced by hypoxia. Reduced levels of transcripts and mitochondrial PHB1 proteins were found in the left ventricle of spontaneously hypertensive rats. Heart-specific PHB1-transgenic mice show low levels of apoptosis and mitochondrial fission in the heart, and consequently, a smaller myocardial infarction size after an experimental infarction [20]. Proteomics studies have shown that PHB1 expression increases dramatically in

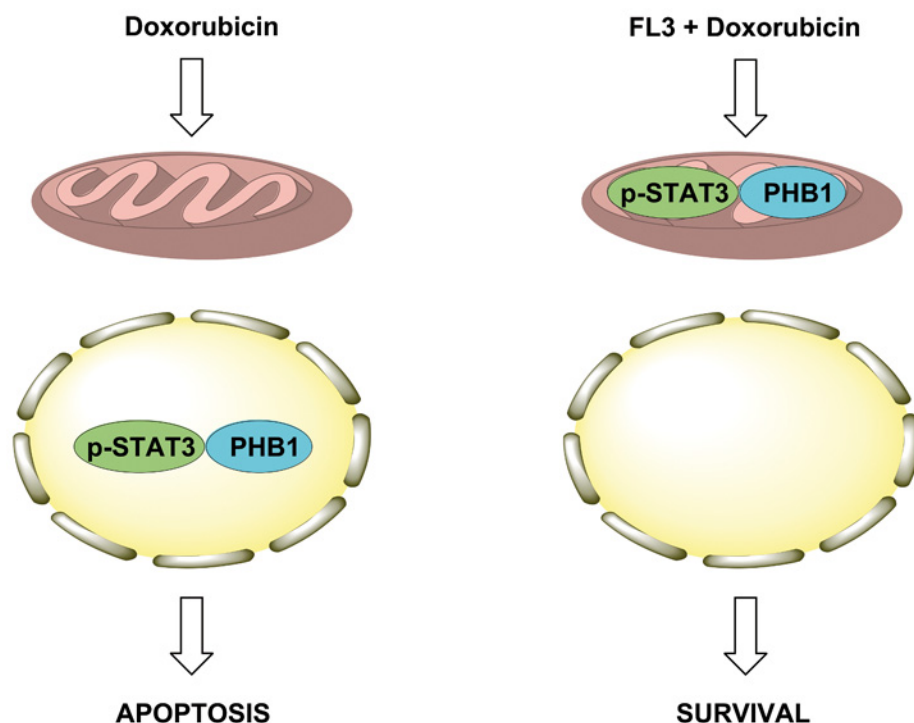


Fig 7. Proposed mechanism of FL3-induced cardioprotection from doxorubicin toxicity. Doxorubicin induces the translocation of PHB1 and phosphorylated STAT3 in the nucleus of cardiomyocytes to induce apoptosis. On the opposite, FL3 induces the translocation of these signaling proteins into mitochondria to protect the cell against the adverse effects of doxorubicin.

doi:10.1371/journal.pone.0141826.g007

cardiomyocytes mitochondria after chronic restraint stress [27]. H₂O₂-induced oxidative stress increases also the mitochondrial content of PHB1 in cardiomyocytes to stabilize mitochondrial membrane potential, inhibit the release of cytochrome c from mitochondria and maintain the mitochondrial function assessed by the preservation of the H⁺-ATPase activity [28]. These data indicate that, in mitochondria, PHB1 is a critical factor that protects cardiomyocytes from oxidative stress.

We found here that in cardiomyocytes, FL3 promotes translocation of PHB1 to mitochondria. This observation is in line with other studies showing that translocation of PHB1 from the nucleus to mitochondria is necessary for cytoprotection in ovarian granulosa cells [23,24], pancreatic β -cells [25], and the retinal epithelium [26]. Accumulation of PHB1 in the mitochondrial membrane can stabilize this membrane, blocking the apoptotic machinery.

Several studies indicate that during apoptosis induced by cytotoxic agents PHB1 migrates to the nucleus where it co-localizes with p53 [29, 30]. Interestingly, we found that doxorubicin does not alter total PHB1 levels in H9c2 cells, but promotes accumulation of PHB1 in the nucleus. This effect was abolished by FL3 treatment, which induced the translocation of PHB1 to mitochondria. The total PHB1 levels in H9c2 cells were also significantly induced by FL3 treatment (for 10h) that was reduced by doxorubicin treatment. The increase of PHB1 expression levels could be due to the activation of STAT3 during the preconditioning by FL3. Indeed, STAT3 is known to upregulate PHB1 during oxidative stress [31].

Theiss and collaborators demonstrated that PHB1 induces phosphorylation of STAT3, thereby stimulating its interaction with PHB1 in mitochondria and ensuring consequent protection of intestinal epithelial cells from TNF- α -induced mitochondrial stress and apoptosis [9]. Such a cytoprotective mechanism has not been reported yet in any other cell types. Consistent with the above observations, our results show that in cardiomyocytes, FL3 induces rapid translocation of PHB1 to mitochondria simultaneously with STAT3 phosphorylation.

STAT3 is a transcription factor that drives expression of antiapoptotic and antioxidant genes [32,33]. STAT3 promotes cardiomyocytes survival through 2 types of actions: -in the nucleus it acts as transcription factor to upregulates iNOS and COX-2 and stimulates the adaptation of the heart to ischemic stress [34]. In mitochondria, STAT3 prevents mitochondria-mediated apoptosis, inhibits the opening of mitochondrial permeability transition pores (MPTP) [32] and modulates the electron transport chain [35]. STAT3 phosphorylation [10] and overexpression [11] have been shown to protect cardiomyocytes from apoptosis induced by doxorubicin in heart tissues.

We demonstrated that inhibition of STAT3 activation by WP1066 blocks the cardioprotective effect of FL3, thus confirming that STAT3 activation is essential for prevention of cardiomyocyte death. The mechanistic link between the activation of STAT3 and PHB1 is currently not clear. Both proteins form a complex in cardiomyocytes 15 min after initiation of FL3 treatment—when STAT3 is maximally phosphorylated—suggesting that both events are connected. It is therefore tempting to hypothesize that STAT3 becomes phosphorylated when it interacts with PHB1, especially because FL3 cannot induce STAT3 phosphorylation or protect cardiomyocytes from doxorubicin toxicity in PHB1-deficient cells.

This study seems to provide the first evidence that targeting of PHB1 by small molecules such as FL3 induces cytoprotection via activation of STAT3 signaling in mitochondria. This strategy may turn out to be a valid therapeutic method for protection of the myocardium from anthracycline-induced cardiotoxicity and ischemia/reperfusion-mediated damage. The beneficial effects of mitochondrial STAT3 in the heart have now been demonstrated, but the currently used methods for activation of mitochondrial STAT3 signaling are not very convenient in terms of clinical application, because of lack of specific activator. Indeed, G-CSF, EPO, and IL-11 protect the heart from ischemic injury, doxorubicin cardiotoxicity, or cardiac fibrosis

utilizing mitochondrial STAT3 signaling pathway, however they also activate other signaling pathways that may induce adverse effects [36–38]. Nevertheless, as far as we know, small molecules, such as FL3, have not been reported to activate STAT3 in the heart.

In summary, mitochondrial versus nuclear PHB/STAT3 complex is critical for the cardio-protective effect of FL3 (Fig 7). Because of the importance of STAT3/PHB1 complex in mitochondria as a therapeutic target in heart failure, the effects of flavaglines need to be examined in experimental models of this disease.

Author Contributions

Conceived and designed the experiments: LD CGN. Performed the experiments: RQ OY AG CB QZ JPW. Analyzed the data: RQ OY AG LD JPW CGN. Contributed reagents/materials/analysis tools: CB QZ. Wrote the paper: LD CGN.

References

1. Vejpongsa P, Yeh ET. Prevention of anthracycline-induced cardiotoxicity: challenges and opportunities. *J Am Coll Cardiol* 2014; 64: 938–945. doi: [10.1016/j.jacc.2014.06.1167](https://doi.org/10.1016/j.jacc.2014.06.1167) PMID: [25169180](https://pubmed.ncbi.nlm.nih.gov/25169180/)
2. Tebbi CK, London WB, Friedman D, Villaluna D, De Alarcon PA, Constine LS, et al. Dexrazoxane-associated risk for acute myeloid leukemia/myelodysplastic syndrome and other secondary malignancies in pediatric Hodgkin's disease. *J Clin Oncol* 2007; 25: 493–500. doi: [10.1200/JCO.2005.02.3879](https://doi.org/10.1200/JCO.2005.02.3879) PMID: [17290056](https://pubmed.ncbi.nlm.nih.gov/17290056/)
3. Basmadjian C, Thuaud F, Ribeiro N, Désaubry L. Flavaglines: potent anticancer drugs that target prohibitins and the helicase eIF4A. *Future Med Chem* 2013; 5: 2185–2197. doi: [10.4155/fmc.13.177](https://doi.org/10.4155/fmc.13.177) PMID: [24261894](https://pubmed.ncbi.nlm.nih.gov/24261894/)
4. Bernard Y, Ribeiro N, Thuaud F, Turkeri G, Dirr R, Boulberdaa M, et al. Flavaglines alleviate doxorubicin cardiotoxicity: implication of Hsp27. *PLoS One* 2011; 6: e25302. doi: [10.1371/journal.pone.0025302](https://doi.org/10.1371/journal.pone.0025302) PMID: [22065986](https://pubmed.ncbi.nlm.nih.gov/22065986/)
5. Ribeiro N, Thuaud F, Bernard Y, Gaidon C, Cresteil T, Hild A, et al. Flavaglines as potent anticancer and cytoprotective agents. *J Med Chem* 2012; 55: 10064–10073. doi: [10.1021/jm301201z](https://doi.org/10.1021/jm301201z) PMID: [23072299](https://pubmed.ncbi.nlm.nih.gov/23072299/)
6. Becker MS, Schmezer P, Breuer R, Haas SF, Essers MA, Krammer PH, et al. The traditional Chinese medical compound Rocaglamide protects nonmalignant primary cells from DNA damage-induced toxicity by inhibition of p53 expression. *Cell Death Dis* 2014; 5: e1000. doi: [10.1038/cddis.2013.528](https://doi.org/10.1038/cddis.2013.528) PMID: [24434508](https://pubmed.ncbi.nlm.nih.gov/24434508/)
7. Polier G, Neumann J, Thuaud F, Ribeiro N, Gelhaus C, Schmidt H, et al. The natural anticancer compounds rocaglamides inhibit the Raf-MEK-ERK pathway by targeting prohibitin 1 and 2. *Chem Biol* 2012; 19: 1093–1104. doi: [10.1016/j.chembiol.2012.07.012](https://doi.org/10.1016/j.chembiol.2012.07.012) PMID: [22999878](https://pubmed.ncbi.nlm.nih.gov/22999878/)
8. Thuaud F, Ribeiro N, Nebigil CG, Désaubry L. Prohibitin ligands in cell death and survival: mode of action and therapeutic potential. *Chem Biol* 2013; 20: 316–331. doi: [10.1016/j.chembiol.2013.02.006](https://doi.org/10.1016/j.chembiol.2013.02.006) PMID: [23521790](https://pubmed.ncbi.nlm.nih.gov/23521790/)
9. Han J, Yu C, Souza RF, Theiss AL. Prohibitin 1 modulates mitochondrial function of Stat3. *Cell Signal* 2014; 26: 2086–2095. doi: [10.1016/j.cellsig.2014.06.006](https://doi.org/10.1016/j.cellsig.2014.06.006) PMID: [24975845](https://pubmed.ncbi.nlm.nih.gov/24975845/)
10. Frias MA, Somers S, Gerber-Wicht C, Opie LH, Lecour S, Lang U. The PGE2-Stat3 interaction in doxorubicin-induced myocardial apoptosis. *Cardiovasc Res* 2008; 80: 69–77. doi: [10.1093/cvr/cvn171](https://doi.org/10.1093/cvr/cvn171) PMID: [18567640](https://pubmed.ncbi.nlm.nih.gov/18567640/)
11. Kunisada K, Negoro S, Tone E, Funamoto M, Osugi T, Yamada S, et al. Signal transducer and activator of transcription 3 in the heart transduces not only a hypertrophic signal but a protective signal against doxorubicin-induced cardiomyopathy. *Proc Natl Acad Sci U S A* 2000; 97: 315–319. doi: [10.1073/pnas.97.1.315](https://doi.org/10.1073/pnas.97.1.315) PMID: [10618415](https://pubmed.ncbi.nlm.nih.gov/10618415/)
12. Jacoby JJ, Kalinowski A, Liu MG, Zhang SS, Gao Q, Chai GX, et al. Cardiomyocyte-restricted knockout of STAT3 results in higher sensitivity to inflammation, cardiac fibrosis, and heart failure with advanced age. *Proc Natl Acad Sci U S A* 2003; 100: 12929–34. doi: [10.1073/pnas.2134694100](https://doi.org/10.1073/pnas.2134694100) PMID: [14566054](https://pubmed.ncbi.nlm.nih.gov/14566054/)
13. Zhu W, Zhang W, Shou W, Field LJ. P53 inhibition exacerbates late-stage anthracycline cardiotoxicity. *Cardiovasc Res* 2014; 103: 81–89. doi: [10.1093/cvr/cvu118](https://doi.org/10.1093/cvr/cvu118) PMID: [24812279](https://pubmed.ncbi.nlm.nih.gov/24812279/)
14. Yano N, Suzuki D, Endoh M, Tseng A, Stabila JP, McGonnigal BG, et al. Beta-adrenergic receptor mediated protection against doxorubicin-induced apoptosis in cardiomyocytes: the impact of high ambient glucose. *Endocrinology* 2008; 149: 6449–6461. doi: [10.1210/en.2008-0292](https://doi.org/10.1210/en.2008-0292) PMID: [18719028](https://pubmed.ncbi.nlm.nih.gov/18719028/)

15. Artal-Sanz M, Tavernarakis N. Prohibitin couples diapause signalling to mitochondrial metabolism during ageing in *C. elegans*. *Nature* 2009; 461: 793–797. doi: [10.1038/nature08466](https://doi.org/10.1038/nature08466) PMID: [19812672](https://pubmed.ncbi.nlm.nih.gov/19812672/)
16. Destouches D, El Khoury D, Hamma-Kourbali Y, Krust B, Albanese P, Katsoris P, et al. Suppression of tumor growth and angiogenesis by a specific antagonist of the cell-surface expressed nucleolin. *PLoS one*. 2008; 3: e2518. doi: [10.1371/journal.pone.0002518](https://doi.org/10.1371/journal.pone.0002518) PMID: [18560571](https://pubmed.ncbi.nlm.nih.gov/18560571/)
17. Thuaud F, Bernard Y, Turkeri G, Dirr R, Aubert G, Cresteil T, et al. Synthetic analogue of rocaglaol displays a potent and selective cytotoxicity in cancer cells: involvement of apoptosis inducing factor and caspase-12. *J Med Chem* 2009; 52: 5176–5187. doi: [10.1021/jm900365v](https://doi.org/10.1021/jm900365v) PMID: [19655762](https://pubmed.ncbi.nlm.nih.gov/19655762/)
18. Theiss AL, Sitaraman SV. The role and therapeutic potential of prohibitin in disease. *Biochim Biophys Acta* 2011; 1813: 1137–1143. doi: [10.1016/j.bbamcr.2011.01.033](https://doi.org/10.1016/j.bbamcr.2011.01.033) PMID: [21296110](https://pubmed.ncbi.nlm.nih.gov/21296110/)
19. Iwamaru A, Szymanski S, Iwado E, Aoki H, Yokoyama T, Fokt I, et al. A novel inhibitor of the STAT3 pathway induces apoptosis in malignant glioma cells both in vitro and in vivo. *Oncogene* 2007; 26: 2435–2444. doi: [10.1038/sj.onc.1210031](https://doi.org/10.1038/sj.onc.1210031) PMID: [17043651](https://pubmed.ncbi.nlm.nih.gov/17043651/)
20. Gratia S, Kay L, Michelland S, Seve M, Schlattner U, Tokarska-Schlattner M. Cardiac phosphoproteome reveals cell signaling events involved in doxorubicin cardiotoxicity. *J Proteomics* 2012; 75: 4705–4716. doi: [10.1016/j.jprot.2012.02.004](https://doi.org/10.1016/j.jprot.2012.02.004) PMID: [22348821](https://pubmed.ncbi.nlm.nih.gov/22348821/)
21. Wang K, Liu CY, Zhang XJ, Feng C, Zhou LY, Zhao Y, et al. miR-361-regulated prohibitin inhibits mitochondrial fission and apoptosis and protects heart from ischemia injury. *Cell Death Differ*. 2015; 22: 1058–1068. doi: [10.1038/cdd.2014.200](https://doi.org/10.1038/cdd.2014.200) PMID: [25501599](https://pubmed.ncbi.nlm.nih.gov/25501599/)
22. Chowdhury I, Thompson WE, Thomas K. Prohibitins role in cellular survival through Ras-Raf-MEK-ERK pathway. *J Cell Physiol* 2014; 229: 998–1004. doi: [10.1002/jcp.24531](https://doi.org/10.1002/jcp.24531) PMID: [24347342](https://pubmed.ncbi.nlm.nih.gov/24347342/)
23. Chowdhury I, Branch A, Olatinwo M, Thomas K, Matthews R, Thompson WE. Prohibitin (PHB) acts as a potent survival factor against ceramide induced apoptosis in rat granulosa cells. *Life Sci* 2011; 89: 295–303. doi: [10.1016/j.lfs.2011.06.022](https://doi.org/10.1016/j.lfs.2011.06.022) PMID: [21763324](https://pubmed.ncbi.nlm.nih.gov/21763324/)
24. Chowdhury I, Thompson WE, Welch C, Thomas K, Matthews R. Prohibitin (PHB) inhibits apoptosis in rat granulosa cells (GCs) through the extracellular signal-regulated kinase 1/2 (ERK1/2) and the Bcl family of proteins. *Apoptosis* 2013; 18: 1513–1525. doi: [10.1007/s10495-013-0901-z](https://doi.org/10.1007/s10495-013-0901-z) PMID: [24096434](https://pubmed.ncbi.nlm.nih.gov/24096434/)
25. Lee JH, Nguyen KH, Mishra S, Nyomba BL. Prohibitin is expressed in pancreatic beta-cells and protects against oxidative and proapoptotic effects of ethanol. *FEBS J* 2010; 277: 488–500. doi: [10.1111/j.1742-4658.2009.07505.x](https://doi.org/10.1111/j.1742-4658.2009.07505.x) PMID: [20030709](https://pubmed.ncbi.nlm.nih.gov/20030709/)
26. Sripathi SR, He W, Atkinson CL, Smith JJ, Liu Z, Elledge BM, et al. Mitochondrial-nuclear communication by prohibitin shuttling under oxidative stress. *Biochemistry* 2011; 50: 8342–8351. doi: [10.1021/bi2008933](https://doi.org/10.1021/bi2008933) PMID: [21879722](https://pubmed.ncbi.nlm.nih.gov/21879722/)
27. Liu XH, Qian LJ, Gong JB, Shen J, Zhang XM, Qian XH. Proteomic analysis of mitochondrial proteins in cardiomyocytes from chronic stressed rat. *Proteomics*. 2004; 4: 3167–76. doi: [10.1002/pmic.200300845](https://doi.org/10.1002/pmic.200300845) PMID: [15378698](https://pubmed.ncbi.nlm.nih.gov/15378698/)
28. Liu X, Ren Z, Zhan R, Wang X, Wang X, Zhang Z, et al. Prohibitin protects against oxidative stress-induced cell injury in cultured neonatal cardiomyocyte. *Cell stress & chaperones*. 2009; 14: 311–9. doi: [10.1007/s12192-008-0086-5](https://doi.org/10.1007/s12192-008-0086-5) PMID: [18958584](https://pubmed.ncbi.nlm.nih.gov/18958584/)
29. Liu YH, Peck K, Lin JY. Involvement of prohibitin upregulation in abrin-triggered apoptosis. Evidence-based complementary and alternative medicine: eCAM. 2012; 2012:605154. doi: [10.1155/2012/605154](https://doi.org/10.1155/2012/605154) PMID: [21961024](https://pubmed.ncbi.nlm.nih.gov/21961024/)
30. Song W, Tian L, Li SS, Shen DY, Chen QX. The aberrant expression and localization of prohibitin during apoptosis of human cholangiocarcinoma Mz-ChA-1 cells. *FEBS letters*. 2014; 588:422–8. doi: [10.1016/j.febslet.2013.12.021](https://doi.org/10.1016/j.febslet.2013.12.021) PMID: [24380853](https://pubmed.ncbi.nlm.nih.gov/24380853/)
31. Jia Y, Zhou F, Deng P, Fan Q, Li C, Liu Y, et al. Interleukin 6 protects H₂O₂-induced cardiomyocytes injury through upregulation of prohibitin via STAT3 phosphorylation. *Cell Biochem Funct* 2012; 30: 426–31. doi: [10.1002/cbf.2820](https://doi.org/10.1002/cbf.2820) PMID: [22431190](https://pubmed.ncbi.nlm.nih.gov/22431190/)
32. Boengler K, Hilfiker-Kleiner D, Drexler H, Heusch G, Schulz R. The myocardial JAK/STAT pathway: from protection to failure. *Pharmacol Ther* 2008; 120: 172–185. doi: [10.1016/j.pharmthera.2008.08.002](https://doi.org/10.1016/j.pharmthera.2008.08.002) PMID: [18786563](https://pubmed.ncbi.nlm.nih.gov/18786563/)
33. Hilfiker-Kleiner D, Hilfiker A, Drexler H. Many good reasons to have STAT3 in the heart. *Pharmacol Ther* 2005; 107: 131–137. doi: [10.1016/j.pharmthera.2005.02.003](https://doi.org/10.1016/j.pharmthera.2005.02.003) PMID: [15963355](https://pubmed.ncbi.nlm.nih.gov/15963355/)
34. Bolli R, Dawn B, Xuan YT. Role of the JAK-STAT pathway in protection against myocardial ischemia/reperfusion injury. *Trends Cardiovasc Med*. 2003; 13: 72–9. PMID: [12586443](https://pubmed.ncbi.nlm.nih.gov/12586443/)
35. Szczepanek K, Chen Q, Larner AC, Lesnfsky EJ. Cytoprotection by the modulation of mitochondrial electron transport chain: the emerging role of mitochondrial STAT3. *Mitochondrion* 2012; 12: 180–189. doi: [10.1016/j.mito.2011.08.011](https://doi.org/10.1016/j.mito.2011.08.011) PMID: [21930250](https://pubmed.ncbi.nlm.nih.gov/21930250/)

36. Harada M, Qin Y, Takano H, Minamino T, Zou Y, Toko H, et al. G-CSF prevents cardiac remodeling after myocardial infarction by activating the Jak-Stat pathway in cardiomyocytes. *Nat Med* 2005; 11: 305–311. doi: [10.1038/nm1199](https://doi.org/10.1038/nm1199) PMID: [15723072](https://pubmed.ncbi.nlm.nih.gov/15723072/)
37. Hoch M, Fischer P, Stapel B, Missol-Kolka E, Sekkali B, Scherr M, et al. Erythropoietin preserves the endothelial differentiation capacity of cardiac progenitor cells and reduces heart failure during anticancer therapies. *Cell Stem Cell* 2011; 9: 131–143. doi: [10.1016/j.stem.2011.07.001](https://doi.org/10.1016/j.stem.2011.07.001) PMID: [21816364](https://pubmed.ncbi.nlm.nih.gov/21816364/)
38. Obana M, Maeda M, Takeda K, Hayama A, Mohri T, Yamashita T, et al. Therapeutic activation of signal transducer and activator of transcription 3 by interleukin-11 ameliorates cardiac fibrosis after myocardial infarction. *Circulation* 2010; 121: 684–691. doi: [10.1161/CIRCULATIONAHA.109.893677](https://doi.org/10.1161/CIRCULATIONAHA.109.893677) PMID: [20100971](https://pubmed.ncbi.nlm.nih.gov/20100971/)